Article

Not peer-reviewed version

Analysing the Cyanobacterial PipX Interaction Network Using NanoBiT Complementation in *Synechococcus elongatus* PCC7942

Carmen Jerez , Antonio Llop , Paloma Salinas , Sirine Bibak , Karl Forchhammer , Asunción Contreras *

Posted Date: 26 March 2024

doi: 10.20944/preprints202403.1501.v1

Keywords: NanoLuc; PII; NtcA; nitrogen regulation; energy regulation; Protein-fragment complementation assays; PCAs; complementation reporter; environmental factors; 2-oxoglutarate

Article

Analysing the Cyanobacterial PipX Interaction Network Using NanoBiT Complementation in *Synechococcus elongatus* PCC7942

Carmen Jerez [1,2], Antonio Llop [1], Paloma Salinas [1], Sirine Bibak [1], Karl Forchhammer [2] and Asunción Contreras [1,*]

[1] Dto. de Fisiología, Genética y Microbiología, Universidad de Alicante, 03690 San Vicente del Raspeig, Spain; carmen.jerez@ua.es; antonio.llop@ua.es; paloma.salinas@ua.es; sb221@alu.ua.es
[2] Interfaculty Institute of Microbiology and Infection Biology, University Tübingen, Auf der Morgenstelle 28, 72076 Tübingen, Germany; karl.forchhammer@uni-tuebingen.de
* Correspondence: contrera@ua.es

Abstract: The conserved cyanobacterial protein PipX is part of a complex interaction network with regulators involved in essential processes that include metabolic homeostasis or ribosome assembly. Because PipX interactions depend on the relative levels of their different partners and of the effector molecules binding to them, *in vivo* studies are required to understand the physiological significance and contribution of environmental factors to regulation of PipX complexes. Here we have used the NanoBiT complementation system to analyse regulation of complex formation in *Synechococcus elongatus* between PipX and each of its two best characterized partners, PII and NtcA. Our results confirm previous *in vitro* analysis on regulation of PipX-PII and PipX-NtcA complexes by 2-oxoglutarate and on regulation of PipX-PII by the ATP/ADP ratio, showing the disruption of PipX-NtcA complexes by increased levels of ADP-bound PII in *Synechococcus elongatus*. The demonstration of a positive role of PII on PipX-NtcA complexes under the initial response to nitrogen starvation or the impact of a PipX point mutation on the activity of PipX-PII and PipX-NtcA reporters are further indications of the sensitivity of the system. This study reveals additional regulatory complexities in the PipX interaction network, opening the way to future research in cyanobacteria.

Keywords: NanoLuc; PII; NtcA; nitrogen regulation; energy regulation; protein-fragment complementation assays; PCAs; complementation reporter; environmental factors; 2-oxoglutarate

1. Introduction

Cyanobacteria, phototrophic prokaryotes that perform oxygenic photosynthesis, constitute an ecologically important phylum that is responsible for the evolution of the oxygenic atmosphere, and are the main contributors to marine primary [1,2]. In addition, their photosynthetic lifestyle and ease of cultivation make them ideal production systems for a number of high-value compounds, including biofuels [3]. Cyanobacteria have developed sophisticated regulatory systems to adapt to the challenging environmental conditions that they face [4,5].

The cyanobacterium *Synechococcus elongatus* PCC 7942 (hereafter *S. elongatus*) is a model system to address fundamental questions concerning the photosynthetic lifestyle. *S. elongatus* is so far the only photosynthetic organism for which the contribution of each gene to fitness has been evaluated [6,7]. Despite important breakthroughs in the genetic analysis of cyanobacteria, there is still a remarkable proportion of genes of unknown function and of unique genes, many of which are presumably involved in functions relevant to the biology of cyanobacteria. One of these unique cyanobacterial proteins is PipX (PII interacting protein X), identified by its ability to form complexes with PII (encoded by *glnB*) and NtcA [8,9], two 2-oxoglutarate (2-OG) sensors having critical roles in carbon/nitrogen homeostasis [10–12].

 doi:10.20944/preprints202403.1501.v1

PII regulates the activity of proteins involved in nitrogen and carbon metabolism in bacteria and plants by direct protein-protein interactions [11], perceiving metabolic information through the competitive binding of ATP or ADP and the synergistic binding of ATP and 2-OG [13–15]. The first PII targets identified in cyanobacteria were NAGK (N-Acetyl Glutamate Kinase) and PipX, detected by yeast two-hybrid approaches in *S. elongatus* [8,9,16]. Their interactions with PII have recently been quantified *in vitro* with unprecedented sensitivity using Split NanoBiT technology [17].

In response to nitrogen limitation, PipX co-activates the regulon of the cyanobacterial global transcriptional regulator NtcA [18,19]. The PipX–NtcA complex consists of one active (2-OG-bound) NtcA dimer and two PipX molecules, each binding to a NtcA subunit [20]. PipX stabilizes the conformation of NtcA that is transcriptionally active and probably helps local recruitment of RNA polymerase. Binding of PipX to PII or NtcA is antagonistically tuned by 2-OG levels: whereas high levels of 2-OG favour the interaction of PipX with NtcA, they prevent the PipX-PII interaction [8,9,20,21].

PipX uses the same surface to bind to either 2-OG-bound NtcA, stimulating DNA binding and transcriptional activity, or to 2-OG-free PII. PII sequestration of PipX at low 2-OG renders PipX unavailable for NtcA binding and activation, reducing the expression of NtcA-dependent gene targets [20–25]. In addition, the interaction between PII and PipX is highly sensitive to fluctuations in the ATP/ADP ratio, and thus the energy state of the cells [26,27].

Diverse studies suggested that PipX forms part of an extended regulatory network beyond NtcA [28–32]. PlmA, a transcriptional regulator found exclusively in cyanobacteria, was identified as a member of the PipX interaction network by yeast three-hybrid searches with PipX–PII as bait [30]. Gradient profiling by sequencing (Grad-seq) showed that PipX co-localizes with either metabolic regulators PII, NtcA and PlmA or with RNA-protein complexes involved in transcription, RNA metabolism and translation initiation [33]. Synteny analysis in cyanobacteria connected PipX with additional proteins [32] one of which was the ribosome-assembly GTPase EngA, whose binding to PipX and regulatory connections in *S. elongatus* have already been demonstrated [29,34].

The regulatory complexity of the PipX interaction network challenges investigations on the physiological significance and the contribution of environmental factors to formation and regulation of the different PipX complexes. Complex formation depends on the relative levels of the different PipX partners and of effector molecules that may bind to them [35], but which are not always known. In this intricated context, maintaining the intracellular environment as untouched as possible should help to address relevant questions on the PipX interaction network.

The NanoBiT complementation system [36], based on reconstitution of the small and high output bioluminescence enzyme NanoLuc, has been used in both mammalian [37–39] and bacterial [40–42] cells to demonstrate the specificity of protein interactions in their natural environment. Very recently, it has been used to study the effect of metabolic fluctuations on interactions mediated by the cyanobacterial PII protein in an *E. coli* host [42]. However, detailed studies of the regulation of complex formation in their natural environment have not been reported.

Here we use the NanoBiT complementation system to analyse regulation of complex formation within the *S. elongatus* interaction network. Our results, in full agreement with the information generated by previous analysis of PipX-PII or PipX-NtcA interactions, reveal additional regulatory complexity. This work constitutes a breakthrough in the field of signaling and interaction networks in cyanobacteria.

2. Results and Discussion

2.1. Reporter Constructs and Strains to Analyse PipX-PII and PipX-NtcA Interactions in S. elongatus

The constructs used here to co-express NanoBiT-based fusion proteins in *S. elongatus* and additional controls are shown in Figure 1. Design of protein fusions was guided by previously validated NanoBiT fusions for *in vitro* assays using the PipX or PII proteins from *Synechocystis* sp. PCC6803 [17]. PipX was fused to the SmBiT fragment (PipX-SmBiT), while PII and NtcA were fused to the LgBiT fragment (PII-LgBiT or NtcA-LgBiT). Flexible linkers of 16 or 8 amino acids, respectively,

 doi:10.20944/preprints202403.1501.v1

were introduced at the C-terminus of PipX or of PII and NtcA. A total of three NSI derivative insertions containing PipX-SmBiT fusions alone or in combination with PII-LgBiT or NtcA-LgBiT were generated. To allow physiological control of the levels of the interacting proteins during environmental changes, the *pipX, glnB* or *ntcA* derivatives were expressed from their corresponding promoter. To facilitate introduction of reporters into the neutral site I (NSI) of the *S. elongatus* chromosome by allelic replacement, a Streptomycin-resistant marker cassette (C.S3) was included within the NSI insertions. The NSI-carrying plasmid pUAGC280 was used as a vector to obtain derivatives containing the relevant insertions, giving plasmids pUAGC1160, pUAGC1161 and pUAGC1163 (Table 1). For simplicity, we will refer hereafter to the NSI derivatives as PipX, PipX-PII or PipX-NtcA constructs or more specifically, as PipX control and PipX-PII or PipX-NtcA reporters.

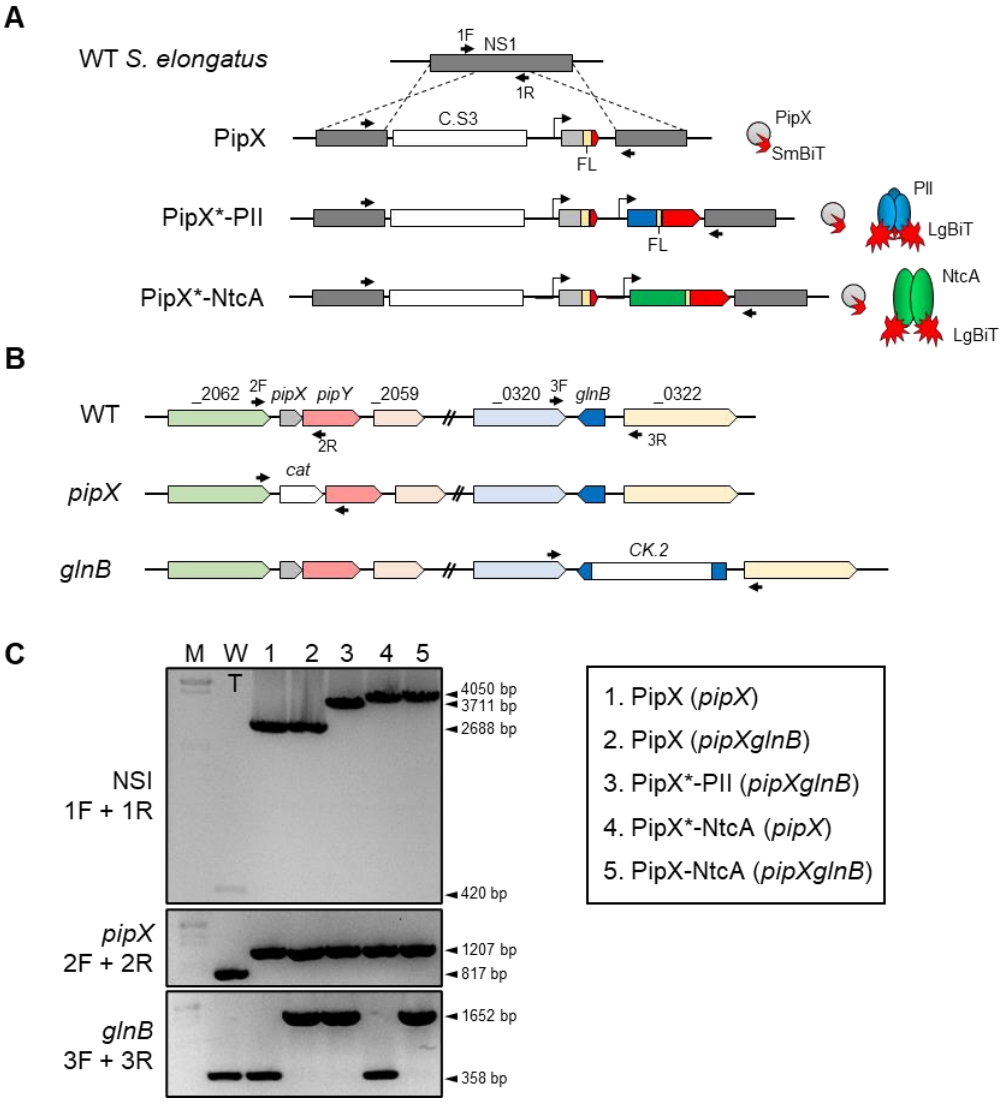

Figure 1. NanoBiT constructs and strategy to analyse PipX-PII and PipX-NtcA interactions in *S. elongatus*. A) The NSI region and derivatives containing the C.S3 selection marker and the corresponding gene fusions are schematically illustrated, with the relevant products depicted at the right. * refers to PipX or PipX^{Y6A}. **B)** Schematic representation of the *pipX* and *glnB* alleles. **C)** Left panel: PCR analysis indicating the primers depicted as black arrows in A and B and size of bands at the left and right, respectively. M: λ *Eco*RI/*Hin*dIII size marker. Right panel: Strains analysed. See text for additional details.

To analyse the impact of a PipX point mutation (Y6A), known to impair contacts with PII and NtcA [20], PipX^{Y6A}-PII and PipX^{Y6A}-NtcA reporters were also generated. Plasmids pUAGC1161 and pUAGC1163 were used to obtain, respectively, plasmids pUAGC1162 and pUAGC1164 (Table 1).

 doi:10.20944/preprints202403.1501.v1

To minimise interference of endogenous proteins with the activity of the NanoBiT reporters and unwanted recombination events in *S. elongatus*, *pipX* and *pipXglnB* null derivatives of *S. elongatus* were chosen as host strains for the PipX or PipX-NtcA constructs and the PipX-PII reporter respectively (Table 2). Although *glnB* is essential in *S. elongatus*, it can be inactivated in a *pipX* background [22,23,25] and, importantly, the *pipX* and *pipXglnB* null mutants show no significant growth defects under constant standard culture conditions [26]. In contrast, *ntcA* is essential in *S. elongatus* in both wild type [6,43] and *pipX* backgrounds, prompting us to use the *pipX* mutant as the default strain for PipX-NtcA reporter analysis. It is worth noting that the potential for interference is greatest for PII due to its abundance [44], its high affinity for PipX [8,20,22,23,25–27] and its trimeric structure, circumstances that would allow it to bind to PipX-SmBiT and/or PII-LgBiT, in detriment of the luciferase signal.

A total of seven strains combining one NanoBiT construct at the NSI site with the inactivation alleles for *pipX* or *pipX* and *glnB* at their original loci were generated during this study (Table 2). In each case, independent streptomycin-resistant clones from each transformation were PCR-analysed to confirm complete segregation of the modified NSI alleles in *S. elongatus* and three validated clones were selected for additional analysis. For simplicity, PCR analysis carried out to verify construction of the strains used in this work have been combined in Figure 1C, and those from Y6A derivative strains, indistinguishable from their wild type counterparts, have been omitted.

Table 1. Plasmids.

Plasmid	Description, relevant characteristics	Reference or source
pUAGC280	P_{trc} into *NSI*, Ap^R Sm^R	[45]
pUAGC1160	(P_{pipX}:*pipX:FL:SmBiT*) into *NSI*, Ap^R Sm^R	This work
pUAGC1161	(P_{pipX}:*pipX:FL:SmBiT* P_{glnB}:*glnB:FL:LgBiT*) into *NSI*, Ap^R Sm^R	This work
pUAGC1162	(P_{pipX}:$pipX^{16ta>gc}$:*FL:SmBiT* P_{glnB}:*glnB:FL:LgBiT*) into *NSI*, Ap^R Sm^R	This work
pUAGC1163	(P_{pipX}:*pipX:FL:SmBiT* P_{ntcA}:*ntcA:FL:LgBiT*) into *NSI*, Ap^R Sm^R	This work
pUAGC1164	(P_{pipX}:$pipX^{16ta>gc}$:*FL:SmBiT* P_{ntcA}:*ntcA:FL:LgBiT*) into *NSI*, Ap^R Sm^R	This work
PII-ST-FL-LgBiT	P_{terR}:PII-StrepTag-FL-LgBiT	[17]
pUAGC126	*pipX* replaced with *cat*, Ap^R Cm^R	[31]
pPM128	*CK2* (+) into *glnB*, Km^R	[46]

Table 2. Strains.

Strain	Genotype, Relevant Characteristics	Reference or Source
E. coli XL1-Blue	*recA1 endA1 gyrA96 thi-1 hsdR17 supE44 relA1* lac [F′ *proAB* $lacI^qZ\Delta M15$ Tn*10* (Tet^R)].	[47]
E. coli TOP10	F^- *mcrA* Δ(*mrr-hsdRMS-mcrBC*) φ80*lacZ*ΔM15 *ΔlacX74 nupG recA1 araD139* Δ(*ara-leu)7697 galE15 galK16 rpsL* (Str^R) *endA1* λ^-	Invitrogen

 doi:10.20944/preprints202403.1501.v1

WT	Wild-type *S. elongatus* PCC7942	Pasteur Culture Collection
pipX	*ΔpipX::cat*, Cm^R	[31]
pipXglnB	*ΔpipX::cat glnB::CK.2*, Cm^R Km^R	[26]
pipX 1^SPipX-SmBiT	*ΔpipX::cat NSI::(P_{pipX}:pipX:FL:SmBiT)*, Sm^R Cm^R	This work
pipXglnB 1^SPipX-SmBiT	*ΔpipX::cat glnB::CK2 NSI::(P_{pipX}:pipX:FL:SmBiT)*, Sm^R Km^R Cm^R	This work
pipXglnB 1^SPipXSmBiT-PIILgBiT	*ΔpipX::cat glnB::CK2 NSI::(P_{pipX}:pipX:FL:SmBiT P_{glnB}:glnB:FL:LgBiT)*, Sm^R Cm^R Km^R	This work
pipXglnB 1^SPipX^{Y6A}SmBiT-PIILgBiT	*ΔpipX::cat glnB::CK2 NSI::(P_{pipX}:pipX$^{16ta>gc}$:FL:SmBiT P_{glnB}:glnB:FL:LgBiT)*, Sm^R Cm^R Km^R	This work
pipX 1^SPipXSmBiT-NtcALgBiT	*ΔpipX::cat NSI::(P_{pipX}:pipX:FL:SmBiT P_{ntcA}:ntcA:FL:LgBiT)*, Sm^R Cm^R	This work
pipX 1^SPipX^{Y6A}SmBiT-NtcALgBiT	*ΔpipX::cat NSI::(P_{pipX}:pipX$^{16ta>gc}$:FL:SmBiT P_{ntcA}:ntcA:FL:LgBiT)*, Sm^R Cm^R	This work
pipXglnB 1^SPipXSmBiT-NtcALgBiT	*ΔpipX::cat glnB::CK2 NSI::(P_{pipX}:pipX:FL:SmBiT P_{ntcA}:ntcA:FL:LgBiT)*, Sm^R Cm^R Km^R	This work

Ap, ampicillin. Km, kanamycin. Sm, streptomycin ^{R}, resistance. Cm, chloramphenicol. Cat, chloramphenicol acetyltransferase.

2.2. PII-LgBiT and PipX-SmBiT Retain Regulatory Features in S. elongatus

Since PipX levels in *S. elongatus* are impaired by mutations decreasing binding to PII or by environmental conditions disrupting PipX-PII complexes [22,25,48], the prediction is that in the absence of PII the levels of PipX would be significantly impaired. To test this idea while seeking evidence that our NanoBiT derivatives maintain regulatory features, we next asked whether the presence of either PII or PII-LgBiT have a positive effect on the levels of PipX-SmBiT.

Western blots with anti-PipX or anti-PII antibodies were carried out from the PipX control or PipX-PII reporter constructs in *S. elongatus* and mutant derivatives. As shown in Figure 2, both PipX-SmBiT and PII-LgBiT were detected in the *pipXglnB* double mutant carrying the PipX-PII reporter construct. While PII-LgBiT was detected at roughly the same levels than PII in the WT strain, the signal detected for PipX-SmBiT was about 15% that of PipX in the WT strain, suggesting that the SmBiT fragment decreases the levels of PipX and/or the affinity for anti-PipX antibody. Importantly, PipX-SmBiT was detected in the *pipX* null strain but not in the *pipXglnB* strain (compare lanes 4-9), thus providing direct evidence of the importance of PII for PipX levels in *S. elongatus*.

 doi:10.20944/preprints202403.1501.v1

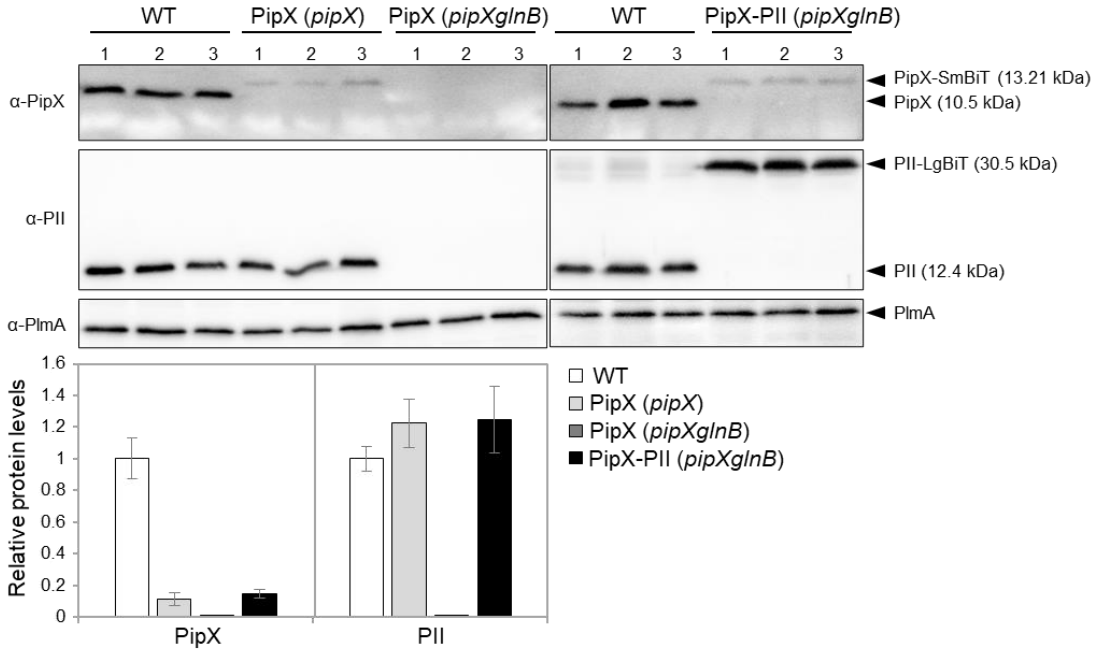

Figure 2. Levels of PipX and PII derivatives in *S. elongatus*. Representative immunodetection of PipX and PII of *S. elongatus* strains differing in the NSI constructs or genetic background (in brackets) as indicated. Relative PipX and PII levels were normalized by the PlmA signal and referred to the WT. Data are presented as means and error bars (standard deviation) from three biological replicates.

Although we cannot rule out that the SmBiT tag interferes with recognition of PipX-SmBiT by the anti-PipX antibody, it is reasonable to assume that the SmBiT tag and/or the ectopic location of the *pipX* gene derivative result in comparatively lower levels of PipX-SmBiT in the PipX-PII reporter strain than levels of PipX in wild type *S. elongatus*. The same would apply to the PipX-NtcA reporter strain. Thus, the reporter strains engineered here would provide informative results with luminescence levels that could potentially be higher.

2.3. PipX-PII and PipX-NtcA Reporters Respond in Opposite Ways to a Drop in the Intracellular ATP Levels in S. elongatus

To test the sensitivity of the NanoBiT PipX-PII and PipX-NtcA reporters to real-time changes in the energy levels, the intracellular ATP/ADP ratio was decreased by adding DCCD, a specific inhibitor of the F_oF_1-ATP synthase [49], to *S. elongatus* cultures growing in standard nitrate medium. The results are shown in Figure 3A alongside schematic illustrations of the relevant players for PipX partner swapping in the analysed strains. These carried PipX-PII or PipX-NtcA reporters in *pipXglnB* or *pipX* backgrounds, respectively.

 doi:10.20944/preprints202403.1501.v1

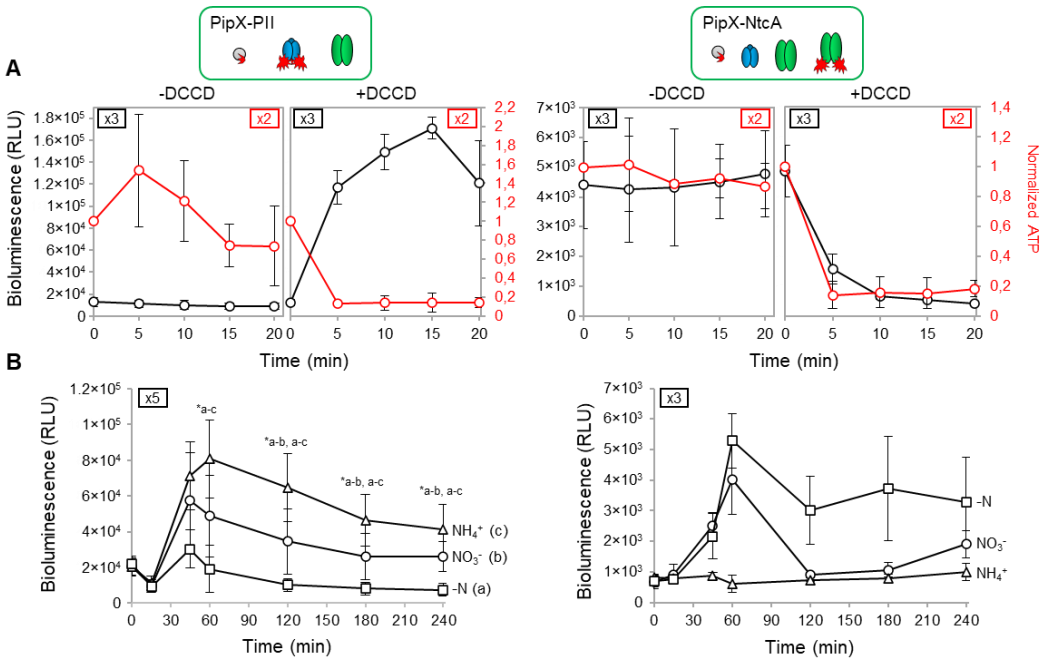

Figure 3. Real-time responses of PipX-PII and PipX-NtcA reporters to changes in energy levels and nitrogen source. Reporter strains are indicated, and relevant proteins illustrated on top of the corresponding results. **A)** Bioluminescence signal (black scale) and normalized ATP levels (red scale) from cultures grown with BG11 in the presence or absence of 200 μM DCCD. **B)** Bioluminescence signal under different nitrogen regimen conditions. Data are presented as means and error bars (standard deviation) from the indicated biological replicates (coloured squares inside the graphics). Wilcoxon rank sum test with Holm–Bonferroni correction between the indicated comparisons produced p-values < 0.05 (*).

Exponentially growing cultures expressing the PipX-PII reporter in the *pipXglnB* background were divided into two before adding DCCD to half of them to record luminescence and intracellular ATP in real-time, at 5 min intervals for up to 20 min (Figure 3A, left). Luminescence values increased (10-fold induction) while a sharp drop at ATP, to approx. 20% of the previous level, took place in the DCCD-containing cultures in less than 5 minutes after addition. Since luminescence and ATP values remained unaltered in the PipX control cultures, the results confirm the sensitivity of the PipX-PII reporter to the intracellular ATP/ADP ratio.

In the case of the PipX-NtcA reporter, the DCCD-containing cultures showed a very fast and strong decrease in luminescence and ATP levels that responded equally to DCCD, dropping to approx. 20% of the previous level (Figure 3A, right). It is worth noting that NtcA does not bind nucleotides and thus the disruption of PipX-NtcA complexes associated to the drop in the ATP/ADP ratio is necessarily indirect. Since it coincides with the drastic increase in luminescence from the PipX-PII reporter, the results must reflect strong competition by PII under these conditions, titrating PipX in detriment of PipX-NtcA complexes.

In summary, the results shown in Figure 3A clearly reflect the direct positive and indirect negative regulation by a low ATP/ADP ratio of PipX-PII and PipX-NtcA complexes, respectively. This is fully consistent with the higher abundance of PII and its very high affinity for PipX, further suggesting that the binding of PipX to its additional targets may also be significantly regulated by the energy levels in *S. elongatus*.

2.4. PipX-PII and PipX-NtcA Reporters Respond in Opposite Ways to 2-OG Levels in S. elongatus

Complex regulation was next analysed under different culture conditions representative of different intracellular levels of the PII effector 2-OG. To obtain low, intermedium or high intracellular 2-OG levels we played with the nitrogen source, adding respectively ammonia, nitrate or no nitrogen

 doi:10.20944/preprints202403.1501.v1

source to the culture media. Nitrate cultures growing at exponential phase were subjected to routine washing protocols before been transferred to fresh media containing either ammonia, nitrate or no added combined nitrogen source. Luminescence was recorded at different timepoints after media transfer for up to 240 min. The results of the analysis are shown in Figure 3B.

For the PipX-PII reporter, during the first half hour after transfer to the different media luminescence values remained below the levels of pre-transfer in all three cultures. Luminescence values significantly increased afterwards, particularly in the ammonium and nitrate cultures, reaching a maximum at the 60′ timepoint, after which they decreased slowly. In contrast, the basal luminescence levels obtained with the PipX control were not affected by the nitrogen source (Figure S1A). Therefore, after an initial period of adaptation (see below), cultures showed the expected inverse correlation between the inferred intracellular carbon to nitrogen ratio (2-OG levels) and PipX-PII binding.

Luminescence from the PipX-NtcA reporter increased after the 15′ timepoint in nitrate and, to a greater extent, in nitrogen deprived cultures, with maximal values obtained at around the 60′ timepoint. As expected, while the basal luminescence levels obtained with the PipX control were not affected by the nitrogen source (Figure S1B), reporter cultures showed a direct correlation between nitrogen scarcity (high 2-OG levels) and PipX-NtcA, particularly for maximal luciferase values. In addition, the oscillation of the reporter signal in conditions in which 2-OG accumulate intracellularly (Figure 3B and S2) is compatible with the existence of a negative feedback-loop counteracting overactivation of NtcA by PipX.

The results shown so far indicate that a) comparison of the real-time luminescence signals from each of the two reporters in each of the three media gave the expected correlations between reporter activity and intracellular 2-OG levels, b) confirmed the reliability and great sensitivity of the NanoBiT system for comparative *in vivo* assays and c) also revealed additional complexities that are further discussed in the following sections.

2.5. PipX Levels Decrease in the Absence of Combined Nitrogen in S. elongatus

While the correlations between reporter activity and the intracellular levels of 2-OG shown in Figure 3 reflect previous knowledge on PipX-PII and PipX-NtcA complexes, the low values of luciferase at the start of the experiment suggested additional regulatory complexity. For instances, reporter signals were always very low after transfer of cultures to fresh media, indicating that the culture manipulations performed during the washing protocol clearly disrupted PipX-PII complexes and additionally delayed formation of new PipX-PII and PipX-NtcA complexes.

Because it is now clear that binding to PII plays a positive role on PipX levels ([48], Figure 2), it appears that disruption of PipX-PII complexes due to high levels of 2-OG during the washing steps may also impair PipX levels. To test this idea, we performed similar washing steps using either nitrogen-free ($BG11_0$) or nitrate-containing (BG11) media in parallel and subsequently determined the levels of PipX in *S. elongatus*. To explore the possible effect of transfer to fresh media we also included a control in which the pellets were resuspended in the same BG11 supernatant.

As shown in Figure 4A, while using the same or new media during the washing protocol appeared irrelevant on PipX levels, these were significantly lower in the cultures washed with $BG11_0$ than in those washed with BG11. Thus, the results further confirm the importance of PipX-PII complexes to maintain PipX levels in *S. elongatus*.

 doi:10.20944/preprints202403.1501.v1

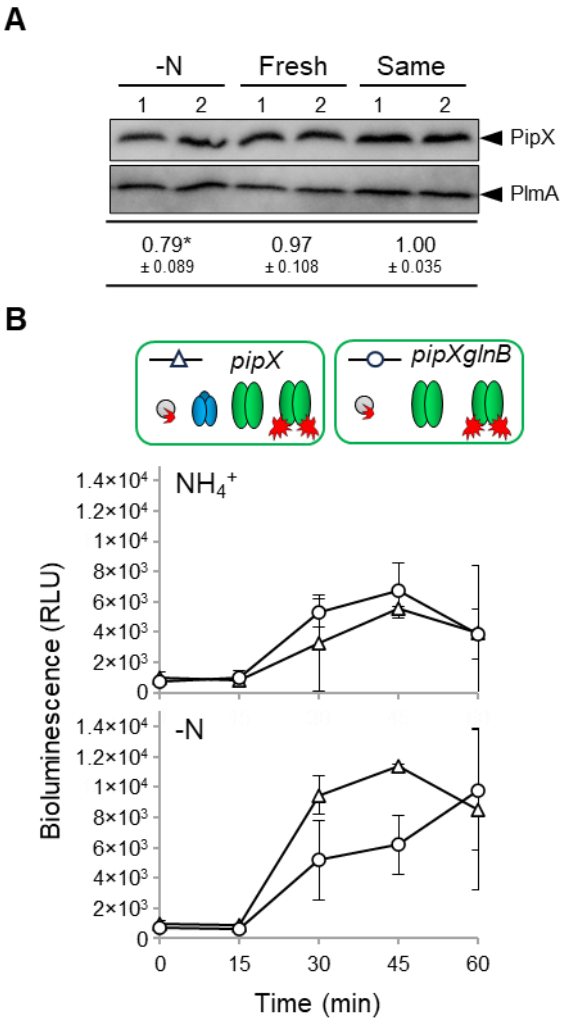

Figure 4. Regulation of PipX levels and PipX-NtcA interactions by PII in response to nitrogen deprivation. A) Representative immunodetection and relative levels of PipX (PipX) from *S. elongatus* cultures after two centrifuge/washing steps with $BG11_0$, BG11 or the same BG11 supernatant (S), normalised to the intensity shown in the same blot by endogenous PlmA, and referred to the S samples. Data are presented as means and error bars (standard deviation) from five biological replicates of two independent experiments. Wilcoxon rank sum test with Holm–Bonferroni correction produced p-values < 0.05 (*) **B)** Real-time comparison of bioluminescence signal under the indicated nitrogen regimens at different times between the *pipX* (Δ) or *pipXglnB* (○) strains. Data are presented as means and error bars (standard deviation) from 2 biological replicates. Other details as in Figure 3.

In summary, the low interaction signals obtained after transfer of cultures to fresh media and the delay to reach maximal bioluminescence signals from both PipX-PII and PipX-NtcA reporters is consistent with the requirement of *de novo* synthesis of PipX.

2.6. PipX Point Mutation Y6A Drastically Impair PipX-PII and PipX-NtcA Complexes in S. elongatus

To provide additional evidence of the sensitivity of the NanoBiT constructs used here, we next analysed the impact of the Y6A mutation on reporter activity. Tyr6 is at the PipX surface, which is involved in contacts with PII and NtcA [20] and its mutation to Ala impairs PipX toxicity, NtcA coactivation [25] and PipX levels [48].

The impact of the Y6A mutation on the activity PipX-PII and PipX-NtcA reporters was determined at timepoint's 0 and 60′ after transfer to ammonia, nitrate or nitrogen-free media. As shown in Figure 5, except for the $PipX^{Y6A}$-PII reporter in ammonium, the levels of activity of the mutant reporters in any given nitrogen regime were indistinguishable from the basal levels obtained

Preprints.org (www.preprints.org) | NOT PEER-REVIEWED | Posted: 26 March 2024 doi:10.20944/preprints202403.1501.v1

with the PipX control constructs. This rather dramatic impact of the Y6A mutation on PipX-PII and PipX-NtcA complexes is consistent with the combined effects of impairing both binding and protein levels in *S. elongatus* and further emphasizes the sensitivity of the NanoBiT system developed here.

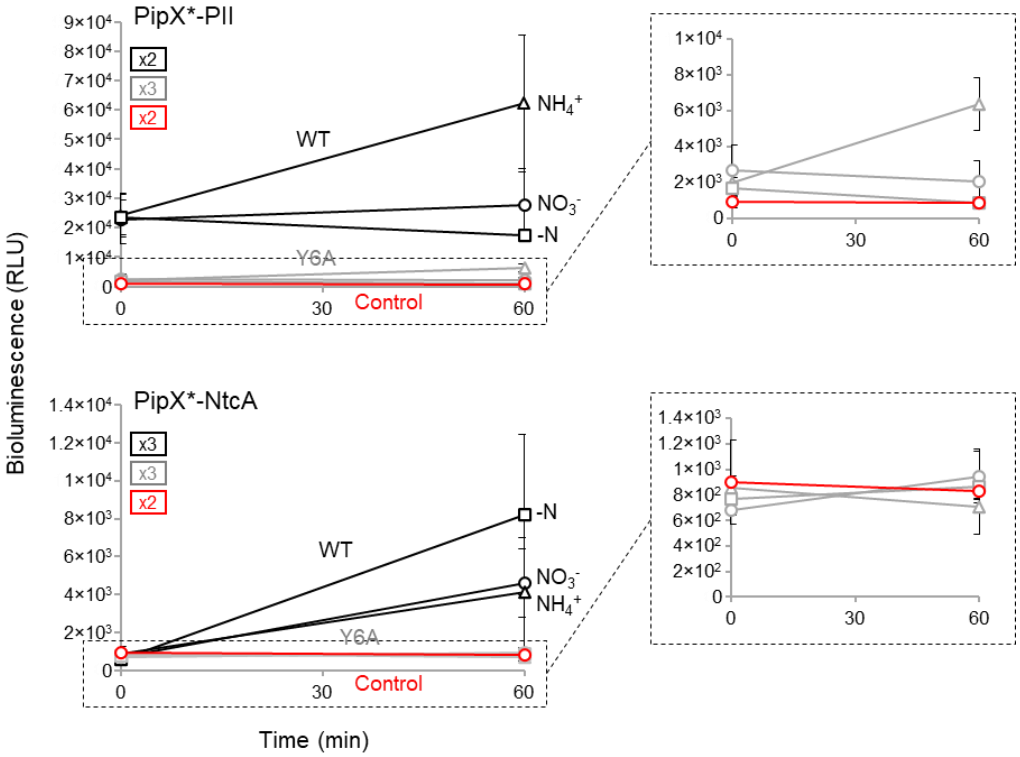

Figure 5. Impact of mutation Y6A on PipX-PII and PipX-NtcA interactions. Bioluminescence signal of the indicated strains under different nitrogen regimen conditions at timepoints 0 and 60'. Black, grey, and red lines indicate WT, Y6A, and control PipX versions, respectively. * refers to PipX or PipX^{Y6A}. Data are presented as means and error bars (standard deviation) from the indicated biological replicates (squares inside the graphics). Inset covers zoom the corresponding region.

2.7. PII Plays a Positive Regulatory Role on PipX-NtcA Complexes under the Initial Response to Nitrogen Deprivation

While it seems clear that in *S. elongatus* PII provides strong competition for PipX-NtcA complexes in nitrate, the role of PII at more extreme 2-OG levels is always assumed to be irrelevant or, given the intracellular abundance of PII, slightly negative over PipX-NtcA complexes. However, the drop in PipX levels observed for BG11$_0$ cultures (Figure 4A) suggested that PII may play a positive role on PipX-NtcA complexes during the response to nitrogen starvation. To test this idea, we transferred nitrate-cultured cells to media with ammonium or without nitrogen source and determined PipX-NtcA reporter activity in *pipX* and *pipXglnB* backgrounds in parallel.

As shown in Figure 4B, no significant differences in luminescence levels were observed between the *pipX* and *pipXglnB* strains after transfer into ammonium-containing media, conditions in which luminescence signals are indistinguishable between the PipX-NtcA and PipX constructs in both *pipX* and *pipXglnB* backgrounds. In contrast, the presence of PII in nitrogen-free cultures was associated with higher luminescence levels during the first 15-45 min after the transfer, consistent with a positive as well as transient role of PII on PipX-NtcA complex formation under conditions of nitrogen-deprivation.

2.8. Additional Players May Affect PipX-PII and PipX-NtcA Complexes in S. elongatus

A consequence of the high sensitivity of our NanoBiT reporter analysis, combined with the regulatory complexity and environmental sensitivity of the biological system used, was that the

 doi:10.20944/preprints202403.1501.v1

absolute values of luminescence levels obtained in *S. elongatus* for a given strain and experimental condition varied depending in which of our laboratories the experiment was performed (data not shown) but also between repetitions of the same experiments on different days under apparently identical conditions. In addition, when bioluminescence levels were just slightly above basal levels, as it happened with the PipX-NtcA reporter when cultures were transferred to ammonium-containing media, the experiments producing lower levels of luminescence were less informative (Figures 3–5 and S1-S2). However, despite all this, the tendencies, response to treatments or the differences between strains being compared was remarkably reproducible. Therefore, rather than integrating data from independent experiments, a representative one with several replicates was shown in each of the figures or tables of this work.

The dynamics of the PipX-PII and PipX-NtcA reporters merit additional comments. The slow decrease of PipX-PII reporter activity after the 60′ timepoint in all three culture conditions shown in Figure 3 seemed to be independent of the nitrogen source and was not accompanied by a reciprocal increase in PipX-NtcA reporter activity, as would be expected if only PII and NtcA would compete for PipX binding. Furthermore, after reaching a maximum at the 60′ timepoint, the PipX-NtcA interaction signal decreased strongly in the nitrate-containing cultures and, given that the 2-OG levels are known to be always higher in nitrate than in ammonium, again the phenomenon appears independent of the nitrogen source, suggesting the involvement of additional regulatory factors. It is thus tempting to propose that a protein binding to PipX may account for these observations.

3. Materials and Methods

3.1. Plasmid and Strain Construction

Plasmids, strains, and oligonucleotides used in this work are listed in Tables 1, 2 and S1, respectively. Cloning procedures were carried out in *Escherichia coli* XL1-Blue or TOP10, using the Gibson assembly cloning method [50]. All constructs were verified using the GATC LIGHTRUN service (Eurofins Genomics, Ebersberg, Germany).

Plasmid pUAGC1160 was obtained by assembling F1 and F2 fragments with the linearized (*Sph*I/*BamH*I) pUAGC280 vector. Fragment F1, comprising *pipX* coding sequence and 141 bp upstream initiation codon, was amplified by PCR from *S. elongatus* genomic DNA with primers CS3-PipX-1F/PipX-FL-1R. Fragment F2, comprising a 16 amino acid flexible linker (FL), as described in [17], and the coding sequence of SmBiT, was generated by PCR using plasmid pUAGC280 as a template with primers NSI-seq/FL-SmBiT-NS1-2F.

Plasmid pUAGC1161 was obtained by assembling F3 and F4 fragments with the linearized (*Bam*HI) pUAGC1160 vector. Fragment F3, comprising *glnB* coding sequence and 187bp upstream of the initiation codon, was amplified by PCR from *S. elongatus* genomic DNA using primers FL-SmBiT-PII-3F/PII-FL-LgBiT-3R. Fragment F4, comprising an 8 amino acids FL, as described in [17], and the coding sequence of LgBiT, was generated by PCR using plasmid PII-ST-FL-LgBiT as a template with primers FL-LgBiT-4F/LgBiT-NS1-4R.

Plasmid pUAGC1163 was obtained by assembling fragments F5 with F6. Fragment F5, comprising the *ntcA* gene and 195 bp upstream of its initiation codon, was amplified by PCR from *S. elongatus* genomic DNA using primers SmBiT-PNtcA-F/NtcA-FL-LgBiT. Fragment F6 was amplified by PCR from pUAGC1161 with primers FL-LgBiT-4F/SmBiT-2R.

Plasmids pUAGC1162 and pUAGC1164 were obtained by Quickchange site-directed mutagenesis (Liu and Naismith, 2008) with primers Y6A-2F/Y6A-2R, and pUAGC1161 and pUAGC1163 as templates, respectively.

To obtain strains expressing PipXSmBiT, PipXSmBiT-NtcALgBiT and PipX^{Y6A}SmBiT-NtcALgBiT in a *pipX* background, and PipXSmBiT-PIILgBiT, PipX^{Y6A}SmBiT-PIILgBiT and PipXSmBiT-NtcALgBiT in a *pipXglnB* background, the required plasmids pUAGC1160, pUAGC1161, pUAG1162, pUAGC1163 or pUAGC1164 were used. Verification of the correct inactivation of *pipX* or *pipXglnB* was confirmed by PCR analysis with oligonucleotide pairs PipX-126-F/PipX-5R and

 doi:10.20944/preprints202403.1501.v1

Glnb-1F/Glnb-1R, respectively. Verification of the correct insertion at the NSI neutral site was confirmed by PCR analysis with oligonucleotide pair NS1-1R/NS1-2R.

3.2. Cyanobacterial Growth and Assays Conditions

S. elongatus cultures were routinely grown at 30°C under constant illumination provided by cool white-fluorescent lights in flasks (70 µmol photons $m^{-2}s^{-1}$; shaking: 150 rpm) or on plates (50 µmol photons $m^{-2}s^{-1}$). The medium used was blue-green algae medium $BG11_0$ (no added nitrogen), BG11 ($BG11_0$ supplemented with 17.5 mM $NaNO_3$ and 10 mM HEPES/NaOH, pH 7.8; [51]) or $BG11_A$ ($BG11_0$ supplemented with 10 mM NH_4Cl and 10 mM HEPES/NaOH, pH 7.8). For solid media, 1.5% (w/v) agar and 0.5 mM sodium thiosulfate ($Na_2S_2O_3$; after autoclaving) were added. Transformations were performed essentially as described in [52]. To select genetically modified strains, solid media were supplemented with the antibiotics chloramphenicol (Cm; 3.5 µg mL^{-1}), streptomycin (Sm; 15 µg mL^{-1}), or kanamycin (Km; 12 µg mL^{-1}). The growth of liquid cultures was monitored by measuring optical density at 750 nm (OD_{750nm}) from 1mL samples using an Ultrospec 2100 pro-UV-Vis Spectrophotometer (Amersham).

To change the nitrogen source, mid-exponential BG11 cultures were harvested by centrifugation (4500×g, 5 min), washed twice with $BG11_0$ and finally resuspended in 20 mL of BG11, $BG11_A$, or $BG11_0$ at a final OD_{750nm} of 0.4 before growing them under standard conditions. To determine the effect of media used during washing steps, the same scheme was followed but washing and resuspending the cells with $BG11_0$, fresh BG11, or their own supernatant BG11. When requiered, DCCD (N, N-dicyclohexylcarbodiimide) to a final concentration of 200 µM was added.

3.3. Bioluminiscence Assays of the NanoBiT Activity and the Intracellular ATP Content

To measure NanoBiT bioluminescence, 500 µL aliquots were mixed with 10 µl of Nano-Glo Live Cell Reagent (Promega) and incubated for 5 minutes under the same culture conditions. The bioluminescence was quantified in a luminometer (Berthold Technologies Junior LB9509) using 10s measuring time. Data was normalized using the OD_{750} of each culture. Values shown in the graphs are represented as RLU (relative luminescence units).

The ATP extraction was essentiality performed as described in [53]. 500 µL aliquots were immediately frozen in liquid nitrogen. ATP was extracted by three consecutive cycles of boiling (100 ºC) and freezing (liquid nitrogen), followed by centrifugation at 14.000 × g for 1 min at 4 ºC. 50 µl of the supernatant was mixed with 50 µl BG11 and 40 µl of a Reaction Solution containing 1 mM DTT, 0.25 mM Luciferin, and 75 µg/ml luciferase from *Photinus pyralis*. The bioluminescence was measured in black 96-well microplates (OptiPlate-96 F HB; PerkinElmer) using a VICTOR3TM 1420 Multilabel Plate Reader (PerkinElmer, Waltham, MA, USA). An ATP standard curve was performed in parallel. Each point was measured twice, the ATP content was quantified using the standard curve, and the data was normalized to the initial point in nitrate (0).

3.4. Protein Extraction, Immunodetection and Band Quantification

Samples of 10 mL from cultures at 0.5-0.7 OD_{750nm} were harvested by 6 min centrifugation at 7300 × g (4 °C) and stored at 20 °C. The pellets were resuspended in 60 µL of lysis buffer (25 mM Tris/HCl pH 7.5, 0.4 mM EDTA, 1 mM DTT, 0.8 mg/mL protease inhibitor, 50 mM NaCl), and cells were disrupted with 1 spoon of 0.1 µm glass beads (≈30 µL), as described in [30]. Mixtures were subjected to three cycles of 60 s at a speed of 5 m/s in a high-speed homogenizer Minibeadbeater, followed by 60 s at 4 °C. Samples were centrifuged (5500 × g for 5 min), and the supernatant fractions (crude protein extracts) were transferred to a new tube. Protein concentrations were estimated by the Bradford method using the PierceTM detergent-compatible Bradford assay kit (ThermoScientific, Waltham, MA, USA) in a VICTOR3TM 1420 Multilabel Plate Reader, and crude protein extracts were stored at −20 °C until needed.

For immunodetection, 60 µg of total protein extract was loaded into a sodium dodecyl sulfate polyacrylamide gel (SDS-PAGE; 15% polyacrylamide). The gel electrophoresis was followed by

 doi:10.20944/preprints202403.1501.v1

immunoblotting onto 0.1 μm polyvinylidene fluoride membranes (from GE Healthcare), and the membranes were subsequently blocked with Tris-Buffered Saline (TBS-Tween; 20 mM Tris/HCl pH 7.5, 500 mM NaCl, Tween 20 0.1%) solution containing 5% non-fat dried milk for 1 h at room temperature, and then incubated overnight in TBS-Tween with 2% non-fat dried milk with the corresponding primary antibody. Membranes were then incubated for 1.5 h at room temperature with a 1:150,000 dilution of ECL rabbit IgG, HRP-linked F(ab')2 fragment (from a donkey; GE Healthcare). The signal was detected with SuperSignal WestFemto reagent (ThermoScientific) in a Biorad ChemiDoc Imager using the automatic exposure mode and avoiding pixel saturation. A 1:5000 dilution of primary anti-PipX, anti-PII, and anti-PlmA antibodies were used separately. Western blot assays were performed for three independent clones of each strain.

Protein intensity levels were quantified from the Western blot images using the ImageJ software version 1.53K. Bands were picked up using the "rectangle" function, and the area plot corresponding to the intensity was measured with the "wand" tool. Each area from the PipX and PII immunodetection was normalised using the corresponding area of PlmA and referred to the control WT strain. Statistical analysis of the results was performed in the RStudio program [54].

4. Conclusions

The purpose of this work has been to gain insight into the complexities and idiosyncrasy of cyanobacterial signal transduction, exemplified here by the alternative and highly regulated association between PipX and its best-known binding partners, the signaling protein PII and the transcriptional regulator NtcA. We have used the NanoBiT complementation system to analyse regulation of PipX-PII and PipX-NtcA complex formation in *S. elongatus*. To provide an intracellular environment as unperturbed as possible, NanoBiT gene fusions maintained their upstream regulatory regions while their endogenous counterparts, except for the essential *ntcA* gene, were deleted to prevent interference with the activity of reporters.

The results obtained here match the wealth of existing information on PipX-PII and PipX-NtcA interactions, their effectors, the relative levels of these three proteins in *S. elongatus* and the effect of point mutations at PipX on complexes. Importantly, they bring new light into the field by showing an exquisite sensitivity of the PipX-PII and PipX-NtcA complexes to specific changes and additional signals, suggesting the existence of an unanticipated negative feedback-loop to tune down over-activation of NtcA by PipX and further revealing that PII exerts a transient role as a NtcA activator, stimulating PipX-NtcA complexes during the initial response to nitrogen deprivation.

In summary, this work expands our knowledge on the complexities of the PipX interaction network and provides, in a model cyanobacterium, a proof of principle for a powerful tool to address the intricacies of signaling and interaction networks.

Supplementary Materials: The following supporting information can be downloaded at the website of this paper posted on Preprints.org, Figure S1: Real-time PipX-SmBiT signal under different nitrogen regimes and backgrounds, Figure S2: Real-time responses of PipX-NtcA reporter to changes in nitrogen source, Table S1: Oligonucleotides, Table S2-S5: Bioluminescence values.

Author Contributions: AC and KF designed research. CJ, SB, AL, and PS performed research. AL performed the statistical analysis. AC wrote the paper. All authors analysed data, contributed to manuscript revision, and read and approved the submitted version.

Funding: This work was supported by grant PID2020-118816GB-I00 funded by MCIN/AEI/10.13039/501100011033 from the Spanish Government, grants VIGROB23-126 and GRE20-04-C from the University of Alicante to AC, and DFG Fo195/21-1 to KF. CJ was the recipient of a Ph.D. fellowship (ACIF/2019/045) from Conselleria d'Innovació, Universitats, Ciència i Societat Digital of the Generalitat Valenciana. SB was supported by a National Grant from the Algerian Ministry of Higher Education and Scientific Research.

Acknowledgments: The authors thank T. Mata for excellent technical support.

Conflicts of Interest: The authors declare no conflict of interest.

References

1. Blank, C.E.; Sánchez-Baracaldo, P. Timing of Morphological and Ecological Innovations in the Cyanobacteria – a Key to Understanding the Rise in Atmospheric Oxygen. *Geobiology* **2010**, *8*, 1–23, doi:10.1111/j.1472-4669.2009.00220.x.
2. Lee, H.-W.; Noh, J.-H.; Choi, D.-H.; Yun, M.; Bhavya, P.S.; Kang, J.-J.; Lee, J.-H.; Kim, K.-W.; Jang, H.-K.; Lee, S.-H. Picocyanobacterial Contribution to the Total Primary Production in the Northwestern Pacific Ocean. *Water (Basel)* **2021**, *13*, 1610, doi:10.3390/w13111610.
3. Khan, S.; Fu, P. Biotechnological Perspectives on Algae: A Viable Option for next Generation Biofuels. *Curr Opin Biotechnol* **2020**, *62*, 146–152, doi:10.1016/j.copbio.2019.09.020.
4. Forchhammer, K.; Selim, K.A. Carbon/Nitrogen Homeostasis Control in Cyanobacteria. *FEMS Microbiol Rev* **2020**, *44*, 33–53, doi:10.1093/femsre/fuz025.
5. Zhang, C.-C.; Zhou, C.-Z.; Burnap, R.L.; Peng, L. Carbon/Nitrogen Metabolic Balance: Lessons from Cyanobacteria. *Trends Plant Sci* **2018**, *23*, 1116–1130, doi:10.1016/j.tplants.2018.09.008.
6. Rubin, B.E.; Wetmore, K.M.; Price, M.N.; Diamond, S.; Shultzaberger, R.K.; Lowe, L.C.; Curtin, G.; Arkin, A.P.; Deutschbauer, A.; Golden, S.S. The Essential Gene Set of a Photosynthetic Organism. *Proceedings of the National Academy of Sciences* **2015**, *112*, E6634-43, doi:10.1073/pnas.1519220112.
7. Welkie, D.G.; Rubin, B.E.; Chang, Y.-G.; Diamond, S.; Rifkin, S.A.; LiWang, A.; Golden, S.S. Genome-Wide Fitness Assessment during Diurnal Growth Reveals an Expanded Role of the Cyanobacterial Circadian Clock Protein KaiA. *Proceedings of the National Academy of Sciences* **2018**, *115*, doi:10.1073/pnas.1802940115.
8. Burillo, S.; Luque, I.; Fuentes, I.; Contreras, A. Interactions between the Nitrogen Signal Transduction Protein PII and *N* -Acetyl Glutamate Kinase in Organisms That Perform Oxygenic Photosynthesis. *J Bacteriol* **2004**, *186*, 3346–3354, doi:10.1128/JB.186.11.3346-3354.2004.
9. Espinosa, J.; Forchhammer, K.; Burillo, S.; Contreras, A. Interaction Network in Cyanobacterial Nitrogen Regulation: PipX, a Protein That Interacts in a 2-oxoglutarate Dependent Manner with PII and NtcA. *Mol Microbiol* **2006**, *61*, 457–469, doi:10.1111/j.1365-2958.2006.05231.x.
10. Esteves-Ferreira, A.A.; Inaba, M.; Fort, A.; Araújo, W.L.; Sulpice, R. Nitrogen Metabolism in Cyanobacteria: Metabolic and Molecular Control, Growth Consequences and Biotechnological Applications. *Crit Rev Microbiol* **2018**, *44*, 541–560, doi:10.1080/1040841X.2018.1446902.
11. Forchhammer, K.; Selim, K.A.; Huergo, L.F. New Views on PII Signaling: From Nitrogen Sensing to Global Metabolic Control. *Trends Microbiol* **2022**, *30*, 722–735, doi:10.1016/j.tim.2021.12.014.
12. Herrero, A.; Muro-Pastor, A.M.; Flores, E. Nitrogen Control in Cyanobacteria. *J Bacteriol* **2001**, *183*, 411–425, doi:10.1128/JB.183.2.411-425.2001.
13. Forchhammer, K.; Hedler, A. Phosphoprotein P_{II} from Cyanobacteria. *Eur J Biochem* **1997**, *244*, 869–875, doi:10.1111/j.1432-1033.1997.00869.x.
14. Huergo, L.F.; Dixon, R. The Emergence of 2-Oxoglutarate as a Master Regulator Metabolite. *Microbiology and Molecular Biology Reviews* **2015**, *79*, 419–435, doi:10.1128/MMBR.00038-15.
15. Kamberov, E.S.; Atkinson, M.R.; Ninfa, A.J. The *Escherichia Coli* PII Signal Transduction Protein Is Activated upon Binding 2-Ketoglutarate and ATP. *Journal of Biological Chemistry* **1995**, *270*, 17797–17807, doi:10.1074/jbc.270.30.17797.
16. Heinrich, A.; Maheswaran, M.; Ruppert, U.; Forchhammer, K. The *Synechococcus Elongatus* P_{II} Signal Transduction Protein Controls Arginine Synthesis by Complex Formation with *N* -acetyl-L -glutamate Kinase. *Mol Microbiol* **2004**, *52*, 1303–1314, doi:10.1111/j.1365-2958.2004.04058.x.
17. Rozbeh, R.; Forchhammer, K. Split NanoLuc Technology Allows Quantitation of Interactions between PII Protein and Its Receptors with Unprecedented Sensitivity and Reveals Transient Interactions. *Sci Rep* **2021**, *11*, 12535, doi:10.1038/s41598-021-91856-2.
18. Espinosa, J.; Rodríguez-Mateos, F.; Salinas, P.; Lanza, V.F.; Dixon, R.; de la Cruz, F.; Contreras, A. PipX, the Coactivator of NtcA, Is a Global Regulator in Cyanobacteria. *Proceedings of the National Academy of Sciences* **2014**, *111*, 201404030–201404097, doi:10.1073/pnas.1404097111.
19. Giner-Lamia, J.; Robles-Rengel, R.; Hernández-Prieto, M.A.; Muro-Pastor, M.I.; Florencio, F.J.; Futschik, M.E. Identification of the Direct Regulon of NtcA during Early Acclimation to Nitrogen Starvation in the Cyanobacterium *Synechocystis* Sp. PCC 6803. *Nucleic Acids Res* **2017**, *45*, 11800–11820, doi:10.1093/nar/gkx860.
20. Llácer, J.L.; Espinosa, J.; Castells, M.A.; Contreras, A.; Forchhammer, K.; Rubio, V. Structural Basis for the Regulation of NtcA-Dependent Transcription by Proteins PipX and PII. *Proceedings of the National Academy of Sciences* **2010**, *107*, 15397–15402, doi:10.1073/pnas.1007015107.
21. Zhao, M.-X.; Jiang, Y.-L.; Xu, B.-Y.; Chen, Y.; Zhang, C.-C.; Zhou, C.-Z. Crystal Structure of the Cyanobacterial Signal Transduction Protein PII in Complex with PipX. *J Mol Biol* **2010**, *402*, 552–559, doi:10.1016/j.jmb.2010.08.006.
22. Espinosa, J.; Castells, M.A.; Laichoubi, K.B.; Contreras, A. Mutations at *pipX* Suppress Lethality of P_{II} -Deficient Mutants of *Synechococcus Elongatus* PCC 7942. *J Bacteriol* **2009**, *191*, 4863–4869, doi:10.1128/JB.00557-09.

23. Espinosa, J.; Castells, M.A.; Laichoubi, K.B.; Forchhammer, K.; Contreras, A. Effects of Spontaneous Mutations in PipX Functions and Regulatory Complexes on the Cyanobacterium *Synechococcus elongatus* Strain PCC 7942. *Microbiology (N Y)* **2010**, *156*, 1517–1526, doi:10.1099/mic.0.037309-0.
24. Forcada-Nadal, A.; Llácer, J.L.; Contreras, A.; Marco-Marín, C.; Rubio, V. The PII-NAGK-PipX-NtcA Regulatory Axis of Cyanobacteria: A Tale of Changing Partners, Allosteric Effectors and Non-Covalent Interactions. *Front Mol Biosci* **2018**, *5*, 91, doi:10.3389/fmolb.2018.00091.
25. Laichoubi, K.B.; Espinosa, J.; Castells, M.A.; Contreras, A. Mutational Analysis of the Cyanobacterial Nitrogen Regulator PipX. *PLoS One* **2012**, *7*, e35845, doi:10.1371/journal.pone.0035845.
26. Espinosa, J.; Labella, J.I.; Cantos, R.; Contreras, A. Energy Drives the Dynamic Localization of Cyanobacterial Nitrogen Regulators during Diurnal Cycles. *Environ Microbiol* **2018**, *20*, 1240–1252, doi:10.1111/1462-2920.14071.
27. Zeth, K.; Fokina, O.; Forchhammer, K. Structural Basis and Target-Specific Modulation of ADP Sensing by the *Synechococcus elongatus* PII Signaling Protein. *Journal of Biological Chemistry* **2014**, *289*, 8960–8972, doi:10.1074/jbc.M113.536557.
28. Cantos, R.; Labella, J.I.; Espinosa, J.; Contreras, A. The Nitrogen Regulator PipX Acts in *cis* to Prevent Operon Polarity. *Environ Microbiol Rep* **2019**, *11*, 495–507, doi:10.1111/1758-2229.12688.
29. Jerez, C.; Salinas, P.; Llop, A.; Cantos, R.; Espinosa, J.; Labella, J.I.; Contreras, A. Regulatory Connections Between the Cyanobacterial Factor PipX and the Ribosome Assembly GTPase EngA. *Front Microbiol* **2021**, *12*, 781760-NA, doi:10.3389/fmicb.2021.781760.
30. Labella, J.I.; Obrebska, A.; Espinosa, J.; Salinas, P.; Forcada-Nadal, A.; Tremiño, L.; Rubio, V.; Contreras, A. Expanding the Cyanobacterial Nitrogen Regulatory Network: The GntR-Like Regulator PlmA Interacts with the PII-PipX Complex. *Front Microbiol* **2016**, *7*, 1677, doi:10.3389/fmicb.2016.01677.
31. Labella, J.I.; Cantos, R.; Espinosa, J.; Forcada-Nadal, A.; Rubio, V.; Contreras, A. PipY, a Member of the Conserved COG0325 Family of PLP-Binding Proteins, Expands the Cyanobacterial Nitrogen Regulatory Network. *Front Microbiol* **2017**, *8*, 1244, doi:10.3389/fmicb.2017.01244.
32. Labella, J.I.; Llop, A.; Contreras, A. The Default Cyanobacterial Linked Genome: An Interactive Platform Based on Cyanobacterial Linkage Networks to Assist Functional Genomics. *FEBS Lett* **2020**, *594*, 1661–1674, doi:10.1002/1873-3468.13775.
33. Riediger, M.; Spät, P.; Bilger, R.; Voigt, K.; Maček, B.; Hess, W.R. Analysis of a Photosynthetic Cyanobacterium Rich in Internal Membrane Systems via Gradient Profiling by Sequencing (Grad-Seq). *Plant Cell* **2021**, *33*, 248–269, doi:10.1093/plcell/koaa017.
34. Llop, A.; Bibak, S.; Cantos, R.; Salinas, P.; Contreras, A. The Ribosome Assembly GTPase EngA Is Involved in Redox Signaling in Cyanobacteria. *Front Microbiol* **2023**, *14*, 1242616-NA, doi:10.3389/fmicb.2023.1242616.
35. Laichoubi, K.B.; Beez, S.; Espinosa, J.; Forchhammer, K.; Contreras, A. The Nitrogen Interaction Network in *Synechococcus* WH5701, a Cyanobacterium with Two PipX and Two PII-like Proteins. *Microbiology (N Y)* **2011**, *157*, 1220–1228, doi:10.1099/mic.0.047266-0.
36. Dixon, A.S.; Schwinn, M.K.; Hall, M.P.; Zimmerman, K.; Otto, P.; Lubben, T.H.; Butler, B.L.; Binkowski, B.F.; Machleidt, T.; Kirkland, T.A.; et al. NanoLuc Complementation Reporter Optimized for Accurate Measurement of Protein Interactions in Cells. *ACS Chem Biol* **2016**, *11*, 400–408, doi:10.1021/acschembio.5b00753.
37. Kashima, D.; Kageoka, M.; Kimura, Y.; Horikawa, M.; Miura, M.; Nakakido, M.; Tsumoto, K.; Nagamune, T.; Kawahara, M. A Novel Cell-Based Intracellular Protein–Protein Interaction Detection Platform (SOLIS) for Multimodality Screening. *ACS Synth Biol* **2021**, *10*, 990–999, doi:10.1021/acssynbio.0c00483.
38. Pipchuk, A.; Yang, X. Using Biosensors to Study Protein–Protein Interaction in the Hippo Pathway. *Front Cell Dev Biol* **2021**, *9*, doi:10.3389/fcell.2021.660137.
39. Sicking, M.; Jung, M.; Lang, S. Lights, Camera, Interaction: Studying Protein–Protein Interactions of the ER Protein Translocase in Living Cells. *Int J Mol Sci* **2021**, *22*, 10358, doi:10.3390/ijms221910358.
40. Bardelang, P.; Murray, E.J.; Blower, I.; Zandomeneghi, S.; Goode, A.; Hussain, R.; Kumari, D.; Siligardi, G.; Inoue, K.; Luckett, J.; et al. Conformational Analysis and Interaction of the Staphylococcus Aureus Transmembrane Peptidase AgrB with Its AgrD Propeptide Substrate. *Front Chem* **2023**, *11*, doi:10.3389/fchem.2023.1113885.
41. Oliveira Paiva, A.M.; Friggen, A.H.; Qin, L.; Douwes, R.; Dame, R.T.; Smits, W.K. The Bacterial Chromatin Protein HupA Can Remodel DNA and Associates with the Nucleoid in Clostridium Difficile. *J Mol Biol* **2019**, *431*, 653–672, doi:10.1016/j.jmb.2019.01.001.
42. Rozbeh, R; Forchhammer, K. *In Vivo* Detection of Metabolic Fluctuations in Real Time Using the NanoBiT Technology Based on PII Signalling Protein Interactions. *Int J Mol Sci* **2024**, *25*, 3409.
43. Espinosa, J.; Forchhammer, K.; Contreras, A. Role of the *Synechococcus* PCC 7942 Nitrogen Regulator Protein PipX in NtcA-Controlled Processes. *Microbiology (N Y)* **2007**, *153*, 711–718, doi:10.1099/mic.0.2006/003574-0.
44. Guerreiro, A.C.L.; Benevento, M.; Lehmann, R.; van Breukelen, B.; Post, H.; Giansanti, P.; Maarten Altelaar, A.F.; Axmann, I.M.; Heck, A.J.R. Daily Rhythms in the Cyanobacterium *Synechococcus elongatus* Probed by

High-Resolution Mass Spectrometry–Based Proteomics Reveals a Small Defined Set of Cyclic Proteins. *Molecular & Cellular Proteomics* **2014**, *13*, 2042–2055, doi:10.1074/mcp.M113.035840.

45. Moronta-Barrios, F.; Espinosa, J.; Contreras, A. Negative Control of Cell Size in the Cyanobacterium *Synechococcus elongatus* PCC 7942 by the Essential Response Regulator RpaB. *FEBS Lett* **2013**, *587*, 504–509, doi:10.1016/j.febslet.2013.01.023.
46. Forchhammer, K.; Tandeau de Marsac, N. Functional Analysis of the Phosphoprotein PII (*glnB* Gene Product) in the Cyanobacterium *Synechococcus* Sp. Strain PCC 7942. *J Bacteriol* **1995**, *177*, 2033–2040, doi:10.1128/jb.177.8.2033-2040.1995.
47. Bullock, W.O.; Fernandez, J.M.; Short, J.M. XL1-Blue—a High-Efficiency Plasmid Transforming *recA Escherichia coli* Strain with β-Galactosidase Selection. *Biotechniques* **1987**, *5*, 376–379.
48. Llop, A.; Tremiño, L.; Cantos, R.; Contreras, A. The Signal Transduction Protein PII Controls the Levels of the Cyanobacterial Protein PipX. *Microorganisms* **2023**, *11*, 2379, doi:10.3390/microorganisms11102379.
49. Takano, S.; Tomita, J.; Sonoike, K.; Iwasaki, H. The Initiation of Nocturnal Dormancy in *Synechococcus* as an Active Process. *BMC Biol* **2015**, *13*, 36, doi:10.1186/s12915-015-0144-2.
50. Gibson, D.G.; Young, L.; Chuang, R.-Y.; Venter, J.C.; Hutchison, C.A.; Smith, H.O. Enzymatic Assembly of DNA Molecules up to Several Hundred Kilobases. *Nat Methods* **2009**, *6*, 343–345, doi:10.1038/nmeth.1318.
51. Rippka, R.; Deruelles, J.; Waterbury, J.B.; Herdman, M.; Stanier, R.Y. Generic Assignments, Strain Histories and Properties of Pure Cultures of Cyanobacteria. *Microbiology (N Y)* **1979**, *111*, 1–61, doi:10.1099/00221287-111-1-1.
52. Taton, A.; Erikson, C.; Yang, Y.; Rubin, B.E.; Rifkin, S.A.; Golden, J.W.; Golden, S.S. The Circadian Clock and Darkness Control Natural Competence in Cyanobacteria. *Nat Commun* **2020**, *11*, 1688, doi:10.1038/s41467-020-15384-9.
53. Doello, S.; Burkhardt, M.; Forchhammer, K. The Essential Role of Sodium Bioenergetics and ATP Homeostasis in the Developmental Transitions of a Cyanobacterium. *Current Biology* **2021**, *31*, 1606-1615.e2, doi:10.1016/j.cub.2021.01.065.
54. RStudio: Integrated Development for R. RStudio 2020. Available online: http://www.rstudio.com/ (accessed on 01 March 2024).